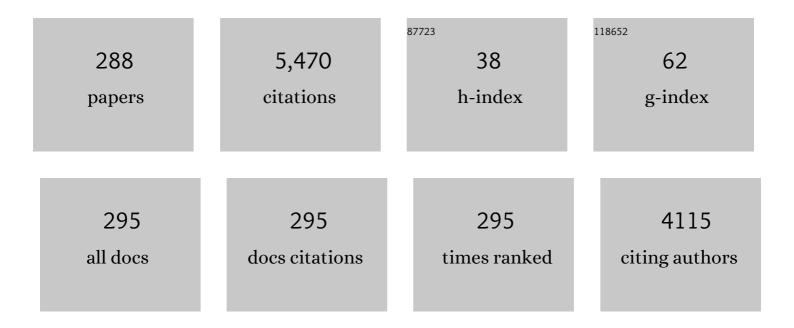
## **Thierry Baudin**

List of Publications by Year in descending order

Source: https://exaly.com/author-pdf/5633352/publications.pdf Version: 2024-02-01



ΤΗΙΕΦΟΥ ΒΛΙΙΠΙΝ

#	Article	IF	CITATIONS
1	Subduction and obduction processes in the Swiss Alps. Tectonophysics, 1998, 296, 159-204.	0.9	299
2	Texture control of 316L parts by modulation of the melt pool morphology in selective laser melting. Journal of Materials Processing Technology, 2019, 264, 21-31.	3.1	258
3	Intermetallic compounds in Al 6016/IF-steel friction stir spot welds. Materials Science & Engineering A: Structural Materials: Properties, Microstructure and Processing, 2010, 527, 4505-4509.	2.6	214
4	Ultrafine grains and the Hall–Petch relationship in an Al–Mg–Si alloy processed by high-pressure torsion. Materials Science & Engineering A: Structural Materials: Properties, Microstructure and Processing, 2012, 532, 139-145.	2.6	141
5	Microstructural evolution in an Al-6061 alloy processed by high-pressure torsion. Materials Science & Engineering A: Structural Materials: Properties, Microstructure and Processing, 2010, 527, 4864-4869.	2.6	119
6	On the role of crystallographic texture in mitigating hydrogen-induced cracking in pipeline steels. Corrosion Science, 2011, 53, 4204-4212.	3.0	116
7	Recrystallization mechanisms in 5251 H14 and 5251 O aluminum friction stir welds. Materials Science & Engineering A: Structural Materials: Properties, Microstructure and Processing, 2007, 445-446, 94-99.	2.6	99
8	Measurement of stored energy in Fe–48%Ni alloys strongly cold-rolled using three approaches: Neutron diffraction, Dillamore and KAM approaches. Materials Science & Engineering A: Structural Materials: Properties, Microstructure and Processing, 2014, 614, 193-198.	2.6	99
9	Simulation of normal grain growth by cellular automata. Scripta Materialia, 1996, 34, 1679-1683.	2.6	96
10	A study on the formation mechanisms of the cube recrystallization texture in cold rolled Fe–36%Ni alloys. Acta Materialia, 2001, 49, 1105-1122.	3.8	93
11	Influence of FSSW parameters on fracture mechanisms of 5182 aluminium welds. Journal of Materials Processing Technology, 2010, 210, 1429-1435.	3.1	92
12	U-Pb zircon (ID-TIMS and SHRIMP) evidence for the early ordovician intrusion of metagranites in the late Proterozoic Canaveilles Group of the Pyrenees and the Montagne Noire (France). Bulletin - Societie Geologique De France, 2005, 176, 269-282.	0.9	91
13	Additive layer manufacturing of titanium matrix composites using the direct metal deposition laser process. Materials Science & Engineering A: Structural Materials: Properties, Microstructure and Processing, 2016, 677, 171-181.	2.6	90
14	EBSD study of hydrogen-induced cracking in API-5L-X46 pipeline steel. Scripta Materialia, 2005, 52, 147-152.	2.6	84
15	Influence of stored energy on twin formation during primary recrystallization. Materials Science & Engineering A: Structural Materials: Properties, Microstructure and Processing, 2014, 589, 112-118.	2.6	83
16	Fertility and Childlessness in the United States. American Economic Review, 2015, 105, 1852-1882.	4.0	81
17	Geochronological constraints on the polycyclic magmatism in the Bou Azzer-El Graara inlier (Central) Tj ETQq1 1	0.78431	4 rgBT /Over

Polycyclic magmatism in the Tagragra d'Akka and Kerdous–Tafeltast inliers (Western Anti-Atlas,) Tj ETQq0 0 0.9 rgBT /Overlock 10 7

#	Article	IF	CITATIONS
19	Evolution of Strength and Homogeneity in a Magnesium AZ31 Alloy Processed by Highâ€Pressure Torsion at Different Temperatures. Advanced Engineering Materials, 2012, 14, 1018-1026.	1.6	74
20	Role of Crystallographic Texture in Hydrogen-Induced Cracking of Low Carbon Steels for Sour Service Piping. Metallurgical and Materials Transactions A: Physical Metallurgy and Materials Science, 2007, 38, 1022-1031.	1.1	70
21	Influence of the Goss grain environment during secondary recrystallisation of conventional grain oriented Fe–3%Si steels. Scripta Materialia, 2002, 47, 725-730.	2.6	68
22	Microstructures and textures of a Cu–Ni–Si alloy processed by high-pressure torsion. Journal of Alloys and Compounds, 2013, 574, 361-367.	2.8	68
23	Investigation of microstructure and texture evolution of a Mg/Al laminated composite elaborated by accumulative roll bonding. Materials Characterization, 2019, 147, 242-252.	1.9	67
24	Influence of the cold rolled reduction on the stored energy and the recrystallization texture in a Fe–53%Ni alloy. Scripta Materialia, 2002, 46, 311-317.	2.6	59
25	Annealing twin formation and recrystallization study of cold-drawn copper wires from EBSD measurements. Materials Characterization, 2007, 58, 947-952.	1.9	57
26	Characterization of Explosive Weld Joints by TEM and SEM/EBSD. Archives of Metallurgy and Materials, 2014, 59, 1129-1136.	0.6	54
27	Formation of annealing twins during primary recrystallization of two low stacking fault energy Ni-based alloys. Journal of Materials Science, 2015, 50, 2167-2177.	1.7	52
28	Shear zone patterns and strain distribution at the scale of a Penninic nappe: the Suretta nappe (Eastern Swiss Alps). Journal of Structural Geology, 1996, 18, 753-764.	1.0	50
29	Effect of aging on microstructural development in an Al–Mg–Si alloy processed by high-pressure torsion. Journal of Materials Science, 2012, 47, 7815-7820.	1.7	47
30	Analysis of laser shock waves and resulting surface deformations in an Al–Cu–Li aluminum alloy. Journal Physics D: Applied Physics, 2012, 45, 335304.	1.3	46
31	New geochemical, geochronological and structural constraints on the Ediacaran evolution of the south Sirwa, Agadir-Melloul and Iguerda inliers, Anti-Atlas, Morocco. Journal of African Earth Sciences, 2014, 98, 47-71.	0.9	46
32	An examination of microstructural evolution in a Cu–Ni–Si alloy processed by HPT and ECAP. Materials Science & Engineering A: Structural Materials: Properties, Microstructure and Processing, 2013, 576, 149-155.	2.6	45
33	Constraints on the Ediacaran inertial interchange true polar wander hypothesis: A new paleomagnetic study in Morocco (West African Craton). Precambrian Research, 2017, 295, 90-116.	1.2	45
34	Texture evolution in high-pressure torsion processing. Progress in Materials Science, 2022, 125, 100886.	16.0	45
35	Shortening of the European Dauphinois margin (Oisans Massif, Western Alps): New insights from RSCM maximum temperature estimates and 40Ar/39Ar in situ dating. Journal of Geodynamics, 2015, 83, 37-64.	0.7	43
36	Basement-cover relationships in the Tambo nappe (Central Alps, Switzerland): geometry, structure and kinematics. Journal of Structural Geology, 1993, 15, 543-553.	1.0	42

#	Article	IF	CITATIONS
37	Experimental study of microstructure changes due to low cycle fatigue of a steel nanocrystallised by Surface Mechanical Attrition Treatment (SMAT). Materials Characterization, 2017, 124, 117-121.	1.9	42

## Zircon U–Pb geochronology of Ordovician magmatism in the polycyclic Ruitor Massif (Internal W) Tj ETQq0 0 0 rgBT /Overlock 10 Tf 5 0.9

39	Texture and microhardness of Mg-Rare Earth (Nd and Ce) alloys processed by high-pressure torsion. Materials Science & Engineering A: Structural Materials: Properties, Microstructure and Processing, 2018, 724, 477-485.	2.6	40
40	Microstructural and textural characterization of copper processed by ECAE. Materials Characterization, 2006, 56, 19-25.	1.9	39
41	Effect of recrystallization and degree of order on the magnetic and mechanical properties of soft magnetic FeCo–2V alloy. Materials Science & Engineering A: Structural Materials: Properties, Microstructure and Processing, 2013, 578, 215-221.	2.6	37
42	Thermal stability of Cu-Cr-Zr alloy processed by equal-channel angular pressing. Materials Characterization, 2016, 118, 527-534.	1.9	37
43	Evaluating the textural and mechanical properties of an Mg-Dy alloy processed by high-pressure torsion. Journal of Alloys and Compounds, 2019, 778, 61-71.	2.8	37
44	Effect of impurities on the recrystallization texture in commercially pure copper-ETP wires. Materials Science & Engineering A: Structural Materials: Properties, Microstructure and Processing, 2007, 456, 261-269.	2.6	36
45	Study of Inconel 718 weldability using MIG CMT process. Science and Technology of Welding and Joining, 2011, 16, 477-482.	1.5	36
46	Monte Carlo simulation of recrystallization in Fe–50%Ni starting from EBSD and bulk texture measurements. Scripta Materialia, 2002, 46, 829-835.	2.6	35
47	Effect of temperature on the processing of a magnesium alloy by high-pressure torsion. Journal of Materials Science, 2012, 47, 7796-7806.	1.7	34
48	Laser cladding of Ni based powder on a Cu-Ni-Al glassmold: Influence of the process parameters on bonding quality and coating geometry. Journal of Alloys and Compounds, 2019, 771, 1018-1028.	2.8	34
49	A ROLE FOR CULTURAL TRANSMISSION IN FERTILITY TRANSITIONS. Macroeconomic Dynamics, 2010, 14, 454-481.	0.6	33
50	Microstructure and texture evolution in a magnesium alloy during processing by high-pressure torsion. Materials Research, 2013, 16, 577-585.	0.6	33
51	Role of microtexture in the interaction and coalescence of hydrogen-induced cracks. Corrosion Science, 2009, 51, 1140-1145.	3.0	32
52	Microstructure, mechanical properties and texture of an AA6061/AA5754 composite fabricated by cross accumulative roll bonding. Materials Science & Engineering A: Structural Materials: Properties, Microstructure and Processing, 2015, 640, 235-242.	2.6	32
53	Microstructural evolution and mechanical properties on an ARB processed IF steel studied by X-ray diffraction and EBSD. Materials Characterization, 2016, 118, 332-339.	1.9	32
54	Relation between the deformation sub-structure after rolling or tension and the recrystallization mechanisms of an IF steel. Materials Science & Engineering A: Structural Materials: Properties, Microstructure and Processing, 2008, 473, 342-354.	2.6	31

#	Article	IF	CITATIONS
55	Texture and microstructure evolution of Fe–Ni alloy after accumulative roll bonding. Journal of Alloys and Compounds, 2014, 610, 352-360.	2.8	31
56	Determination of the total texture. Metallurgical and Materials Transactions A - Physical Metallurgy and Materials Science, 1993, 24, 2299-2311.	1.4	29
57	Geodynamic evolution of a wide plate boundary in the Western Mediterranean, near-field <i>versus</i> far-field interactions. Bulletin - Societie Geologique De France, 2021, 192, 48.	0.9	29
58	On the non-existence of a Cadomian basement in southern France (Pyrenees, Montagne Noire): implications for the significance of the pre-Variscan (pre-Upper Ordovician) series. Bulletin - Societie Geologique De France, 2004, 175, 643-655.	0.9	28
59	Basement shear zones development and shortening kinematics in the Ecrins Massif, Western Alps. Tectonics, 2014, 33, 84-111.	1.3	28
60	Observations of and model for insular grains and grain clusters formed during anomalous grain growth in N18 superalloy. Journal of Applied Physics, 1998, 84, 6366-6371.	1.1	26
61	Characterization at a local scale of a laser-shock peened aluminum alloy surface. Applied Surface Science, 2011, 257, 7195-7203.	3.1	26
62	Microstructure and texture evolution during the ultra grain refinement of the Armco iron deformed by accumulative roll bonding (ARB). Materials Science & Engineering A: Structural Materials: Properties, Microstructure and Processing, 2013, 561, 60-66.	2.6	26
63	Religion and fertility: The French connection. Demographic Research, 0, 32, 397-420.	2.0	26
64	Microstructural characterization in a hot-rolled, two-phase steel. Materials Characterization, 2001, 47, 365-373.	1.9	25
65	Stored energy evolution in both phases of a duplex steel as a function of cold rolling reduction. Scripta Materialia, 2006, 54, 683-688.	2.6	25
66	Orientation changes inside shear bands occurring in channel-die compressed (112)[1Ì,,1Ì,,1]copper single crystals. Scripta Materialia, 1996, 35, 397-403.	2.6	24
67	Microstructure and texture evolution in a Cu–Ni–Si alloy processed by equal-channel angular pressing. Journal of Alloys and Compounds, 2015, 638, 88-94.	2.8	24
68	On the evolution of microstructure, texture and corrosion behavior of a hot-rolled and annealed AZ31 alloy. Materials Chemistry and Physics, 2021, 267, 124598.	2.0	24
69	"in-situ―neutron diffraction study of the cube crystallographic texture development in Fe53%-Ni alloy during recrystallization. Scripta Materialia, 2000, 43, 325-330.	2.6	23
70	Simulation of primary recrystallization from tem orientation data. Scripta Materialia, 2000, 43, 63-68.	2.6	22
71	Influence of neighbourhood on abnormal Goss grain growth in Fe–3% Si steels: Formation of island grains in the large growing grain. Scripta Materialia, 2006, 55, 641-644.	2.6	22
72	Peneplanation and lithosphere dynamics in the Pyrenees. Comptes Rendus - Geoscience, 2016, 348, 194-202.	0.4	22

#	Article	IF	CITATIONS
73	Contribution to the analysis of the $\hat{I}\pm/\hat{I}^2$ interface in some titanium alloys. Journal of Materials Research, 1991, 6, 987-998.	1.2	21
74	TEM study of recovery and recrystallization mechanisms after 40% cold rolling in an IF-Ti steel. Scripta Materialia, 2005, 53, 1001-1006.	2.6	21
75	Texture evolution of an Fe–Ni alloy sheet produced by cross accumulative roll bonding. Materials Characterization, 2014, 97, 140-149.	1.9	21
76	An EBSD analysis of Fe-36%Ni alloy processed by HPT at ambient and a warm temperature. Journal of Alloys and Compounds, 2018, 753, 46-53.	2.8	21
77	Thermal Stability of an Mg–Nd Alloy Processed by Highâ€Pressure Torsion. Advanced Engineering Materials, 2019, 21, 1900801.	1.6	21
78	Deformation textures in wire drawn perlitic steel. International Journal of Material Forming, 2010, 3, 7-11.	0.9	20
79	Elaboration and structural characterization of glasses inside the ternary SrO-TiO2-P2O5 system. Journal of Physics and Chemistry of Solids, 2012, 73, 961-968.	1.9	20
80	Microstructural and textural investigation of an Mg–Dy alloy after hot plane strain compression. Journal of Magnesium and Alloys, 2020, 8, 1198-1207.	5.5	20
81	3D Modeling and Kinematics of the External Zone of the French Western Alps (Belledonne and Grand) Tj ETQq1	1 0,784314 0.6	l rgBT /Overl
82	Early Stages of Recrystallization in Equal-Channel Angular Pressing (ECAP)-Deformed AA3104 Alloy Investigated Using Scanning Electron Microscopy (SEM) and Transmission Electron Microscopy (TEM) Orientation Mappings. Metallurgical and Materials Transactions A: Physical Metallurgy and Materials Science, 2012, 43, 4777-4793.	1.1	19
83	Barkhausen noise measurements give direct observation of magnetocrystalline anisotropy energy in ferromagnetic polycrystals. Journal Physics D: Applied Physics, 2013, 46, 392001.	1.3	19
84	EBSD study of the development of cube recrystallization texture in Fe–50%Ni. Scripta Materialia, 2001, 45, 413-420.	2.6	18
85	Simulation of primary recrystallization from TEM observations and neutron diffraction measurements. Scripta Materialia, 2004, 51, 427-430.	2.6	18
86	<i>In Situ</i> Electron Backscatter Diffraction Investigation of Recrystallization in a Copper Wire. Microscopy and Microanalysis, 2013, 19, 969-977.	0.2	18
87	On the stored energy evolution after accumulative roll-bonding of invar alloy. Materials Chemistry and Physics, 2017, 201, 408-415.	2.0	18
88	Estimation of the Minimum Grain Number for the Orientation Distribution Function Calculation from Individual Orientation Measurements on Fe–3%Si and Ti–4Al–6V Alloys. Journal of Applied Crystallography, 1995, 28, 582-589.	1.9	17
89	Grain growth simulation starting from experimental data. Scripta Materialia, 1997, 36, 789-794.	2.6	17
90	Reinforcement of the Cube texture during recrystallization of a 1050 aluminum alloy partially recrystallized and 10% cold-rolled. Materials Characterization, 2012, 64, 1-7.	1.9	17

#	Article	IF	CITATIONS
91	On the evaluation of dislocation densities in pure tantalum from EBSD orientation data. Materiaux Et Techniques, 2018, 106, 604.	0.3	17
92	Primary Recrystallization of Invar, Feâ€36%Ni Alloy: Origin and Development of the Cubic Texture. Advanced Engineering Materials, 2010, 12, 1047-1052.	1.6	15
93	Quantitative infrared analysis of welding processes: temperature measurement during RSW and CMT-MIG welding. Science and Technology of Welding and Joining, 2014, 19, 38-43.	1.5	15
94	The effect of Ti/Y ratio on the recrystallisation behaviour of Fe–14%Cr oxide dispersion-strengthened alloys. Journal of Nuclear Materials, 2014, 452, 359-363.	1.3	15
95	Comparison of four arc welding processes used for aluminium alloy cladding. Science and Technology of Welding and Joining, 2015, 20, 75-81.	1.5	15
96	An investigation of the stored energy and thermal stability in a Cu–Ni–Si alloy processed by high-pressure torsion. Philosophical Magazine, 2020, 100, 688-712.	0.7	15
97	Basementâ€Cover Decoupling During the Inversion of a Hyperextended Basin: Insights From the Eastern Pyrenees. Tectonics, 2021, 40, e2020TC006512.	1.3	15
98	Monte Carlo simulation of primary recrystallization and annealing twinning. Acta Materialia, 2014, 81, 457-468.	3.8	14
99	Effect of long range order on mechanical properties of partially recrystallized Fe49Co–2V alloy. Materials Science & Engineering A: Structural Materials: Properties, Microstructure and Processing, 2014, 592, 70-76.	2.6	14
100	Compromise between magnetic shielding and mechanical strength of thin Al/Steel/Al sandwiches produced by cold roll bonding: Experimental and numerical approaches. Journal of Alloys and Compounds, 2019, 798, 67-81.	2.8	14
101	Simulation of the anisotropic growth of goss grains in Fe3%Si sheets (grade HiB). Scripta Materialia, 1999, 40, 1111-1116.	2.6	13
102	Sur l'origine karstique et l'âge plio-quaternaire des accumulations bréchiques dites «brèches marin et paléocA¨nes» d'Amélie-les-Bains (Pyrénées-Orientales, France). Eclogae Geologicae Helveticae, 2 99, 49-64.		13
103	In Situ EBSD Investigation of Recrystallization in a Partially Annealed and Coldâ€Rolled Aluminum Alloy of Commercial Purity. Advanced Engineering Materials, 2012, 14, 39-44.	1.6	13
104	Texture and grain size dependence of grain boundary character distribution in recrystallized Fe-50%Ni. Scripta Materialia, 1999, 41, 847-853.	2.6	12
105	Comparison between recrystallization mechanisms in copper and Ti-IF steel after a low amount of deformation. Materials Science & Engineering A: Structural Materials: Properties, Microstructure and Processing, 2011, 528, 3829-3832.	2.6	12
106	Accumulative Roll Bonding at Room Temperature of a Biâ€Metallic AA5754/AA6061 Composite: Impact of Strain Path on Microstructure, Texture, and Mechanical Properties. Advanced Engineering Materials, 2018, 20, 1700285.	1.6	12
107	Effect of heat treatment on the mechanical properties and microstructure of HSLA steels processed by various technologies. Materials Today Communications, 2021, 28, 102598.	0.9	12
108	Selective electrodeposition of PbO2 on anodised-polycrystalline titanium. Electrochimica Acta, 2004, 49, 2369-2377.	2.6	11

#	Article	IF	CITATIONS
109	Neutron Diffraction Measurements of Deformation and Recrystallization Textures in Cold Wire-Drawn Copper. Materials Science Forum, 2005, 495-497, 919-926.	0.3	11
110	Dynamic Recrystallization Modeling during Hot Forging of a Nickel Based Superalloy. Materials Science Forum, 0, 638-642, 2321-2326.	0.3	11
111	The deformation and recrystallization behaviour of an Mg-Dy alloy processed by plane strain compression. Materials Today Communications, 2020, 24, 101239.	0.9	11
112	Orientation correlations in primary recrystallized Fe-50%Ni. Materials Science & Engineering A: Structural Materials: Properties, Microstructure and Processing, 2001, 298, 227-234.	2.6	10
113	Texture Evolution in Invar <sup>®</sup> Deformed by Asymmetrical Rolling. Materials Science Forum, 2007, 550, 551-556.	0.3	10
114	The Effect of the Strain Path and the Second Phase Particles on the Microstructure and the Texture Evolution of the AA3104 Alloy Processed by ECAP. Archives of Metallurgy and Materials, 2011, 56, .	0.6	10
115	Microstructural Evolution and Texture Analysis in a Thermomechanically Processed Low SFE Superâ€Austenitic Steel (Alloyâ€28). Advanced Engineering Materials, 2018, 20, 1700928.	1.6	10
116	A stored energy analysis of grains with shear texture orientations in Cu-Ni-Si and Fe-Ni alloys processed by high-pressure torsion. Journal of Alloys and Compounds, 2021, 864, 158142.	2.8	10
117	Development of the PC-GMAW welding technology for TMCP steel in accordance with welding thermal cycle, welding technique, structure, and properties of welded joints. Reports in Mechanical Engineering, 2020, 1, 26-33.	4.9	10
118	Impurities Effects on the Stored Elastic Energy in Cold-drawn Copper Wires. Journal of Neutron Research, 2004, 12, 249-254.	0.4	9
119	A Study of Local Microstructure and Texture Heterogeneities in a CGO Fe3%Si Alloy from Hot Rolling to Primary Recrystallization. Materials Science Forum, 2005, 495-497, 483-488.	0.3	9
120	Effect of TiO2 and SrO additions on some physical properties of 33Na2O–xSrO–xTiO2–(50Ââ^'Â2x)B2O3–17P2O5 glasses. Journal of Thermal Analysis and Calorimetry, 2 111, 401-408.	2013,	9
121	Study of the Relation between Microstructure and Properties (Mechanical/Electrical) of Copper Wire Drawing and Annealed. Acta Physica Polonica A, 2013, 123, 470-472.	0.2	9
122	Relaxation path of nanoparticles in an oxygen-enriched ferritic oxide-dispersion-strengthened alloy. Scripta Materialia, 2017, 136, 37-40.	2.6	9
123	Magnetic Shielding at Low Frequencies: Application for an Aluminum/Steel Composite Elaborated by Accumulative Roll Bonding. Advanced Engineering Materials, 2019, 21, 1800967.	1.6	9
124	Welding Thermal Cycle Impact on the Microstructure and Mechanical Properties of Thermo–Mechanical Control Process Steels. Steel Research International, 2021, 92, 2000645.	1.0	9
125	Comparison of several methods for the reproduction of the orientation distribution function from pole figures in medium to strong textured materials. EPJ Applied Physics, 2001, 15, 85-96.	0.3	8
126	Study of the development of the cube texture in Fe-50%Ni during recrystallization and normal grain growth. EPJ Applied Physics, 2002, 20, 77-89.	0.3	8

#	Article	IF	CITATIONS
127	Title is missing!. Journal of Materials Science, 2002, 10, 303-309.	1.2	8
128	Microstructural Changes in Copper Processed by Equal Channel Angular Extrusion and Static Annealing. Materials Science Forum, 2003, 426-432, 2723-2728.	0.3	8
129	Monte Carlo Method for Simulating Grain Growth in 3D Influence of Lattice Site Arrangements. Materials Science Forum, 2004, 467-470, 1117-1122.	0.3	8
130	Strain-induced dissolution of Y–Ti–O nano-oxides in a consolidated ferritic oxide dispersion strengthened (ODS) steel. Materialia, 2018, 4, 444-448.	1.3	8
131	Microstructural Evolutions and Mechanical Properties of Drawn Medium Carbon Steel Wire. International Journal of Engineering Research in Africa, 0, 41, 1-7.	0.7	8
132	Probabilistic and deterministic full field approaches to simulate recrystallization in ODS steels. Computational Materials Science, 2020, 179, 109646.	1.4	8
133	Optimization of the pulsed arc welding parameters for wire arc additive manufacturing in austenitic steel applications. International Journal of Advanced Manufacturing Technology, 2022, 119, 5175-5193.	1.5	8
134	Characterization of Recrystallization Textures in Fe-3% Si Sheets by EBSP: Comparison With X Ray Diffraction. Textures and Microstructures, 1991, 14, 597-610.	0.2	7
135	Deformation textures and plastic anisotropy of steels using the Taylor and nonhomogeneous models. International Journal of Plasticity, 1994, 10, 643-661.	4.1	7
136	Automatic Orientation Measurements in TEM for Studying Fe-Ni Recrystallization Mechanisms. Materials Science Forum, 2002, 408-412, 523-528.	0.3	7
137	Texture and Evolution of Recrystallization in Low Carbon Steel Wire. Materials Science Forum, 2006, 514-516, 554-558.	0.3	7
138	INCONEL 718 Recrystallization in the Delta Supersolvus Domain. Advanced Materials Research, 0, 409, 751-756.	0.3	7
139	Microstructure and microtexture evolution with aging treatment in an Al–Mg–Si alloy severely deformed by HPT. Journal of Materials Science, 2013, 48, 4573-4581.	1.7	7
140	Recrystallization texture development by multiple twinning in the Invar (Fe-36 %Ni) alloy. Revue De Metallurgie, 2003, 100, 193-202.	0.3	6
141	Estimation of Stored Energy Distribution from EBSD Measurements. Materials Science Forum, 2004, 467-470, 51-56.	0.3	6
142	Temperature and Deformation Effects on the Recrystallization Microstructure and Texture of Wire Draw Steel. Materials Science Forum, 2007, 550, 447-452.	0.3	6
143	In-situ EBSD investigation of thermal stability of a 316L stainless steel nanocrystallized by Surface Mechanical Attrition Treatment. Materials Letters, 2020, 263, 127249.	1.3	6
144	Characterization of untransformed ferrite in 10Cr and 12Cr ODS steels. Materialia, 2021, 16, 101066.	1.3	6

#	Article	IF	CITATIONS
145	Effect of ECAP and Subsequent Annealing on Microstructure, Texture, and Microhardness of an AA6060 Aluminum Alloy. Journal of Materials Engineering and Performance, 2022, 31, 2606-2623.	1.2	6
146	Microtexture determination in Fe–Si alloy sheets by etch pitting. Comparison with the electron back-scattering pattern technique. Journal of Applied Crystallography, 1994, 27, 924-933.	1.9	5
147	Percolation Properties of Internal Wetted Polycrystals: Effect of Stresses and Material Structure. Materials Science Forum, 2002, 404-407, 373-380.	0.3	5
148	Formation and Control of the Cube Texture in Fe-Ni Alloys. Materials Science Forum, 2002, 408-412, 739-748.	0.3	5
149	Study of Deformation Microstructure and Static Recovery in Copper after Cold Drawing. Materials Science Forum, 2004, 467-470, 27-32.	0.3	5
150	Monte Carlo Modeling of Low Carbon Steel Recrystallization: Role of Thermo-Mechanical Treatment and Chemical Composition. Materials Science Forum, 2005, 495-497, 507-512.	0.3	5
151	Microstructural Evolution in an Al-6061 Alloy Processed by High-Pressure Torsion and Rapid Annealing. Materials Science Forum, 0, 667-669, 223-228.	0.3	5
152	The Optimal Trade-Off Between Quality and Quantity with Unknown Number of Survivors. Mathematical Population Studies, 2012, 19, 94-113.	0.8	5
153	Influence of Sulfur on the Recrystallization and {100}ã€^001〉 Cube Texture Formation in Fe48%Ni Alloys Tapes. Advanced Engineering Materials, 2014, 16, 933-939.	1.6	5
154	Comparison between ARB and CARB processes on an AA5754/AA6061 composite. IOP Conference Series: Materials Science and Engineering, 2014, 63, 012090.	0.3	5
155	Grain boundary character distribution of CuNiSi and FeNi alloys processed by severe plastic deformation. IOP Conference Series: Materials Science and Engineering, 2015, 82, 012076.	0.3	5
156	EBSD characterization of an IF steel processed by Accumulative Roll Bonding. IOP Conference Series: Materials Science and Engineering, 2015, 82, 012077.	0.3	5
157	Effect of Annealing Atmosphere on the Recrystallized Texture and Abnormal Grain Growth of Ni–5%W Alloy Sheets. Advanced Engineering Materials, 2015, 17, 1568-1572.	1.6	5
158	The Influence of Aging on Industrially Cold Drawn Aluminum Alloy (6101) Used in the Electric Transmission Lines. International Journal of Engineering Research in Africa, 2016, 24, 9-16.	0.7	5
159	Study of the microstructure and texture heterogeneities of Fe–48wt%Ni alloy severely deformed by equal channel angular pressing. Journal of Materials Science, 2019, 54, 4354-4365.	1.7	5
160	Mechanical Properties and Texture Evolution of High-Carbon Steel Wires during Wire Drawing: Strand Manufacturing. International Journal of Engineering Research in Africa, 0, 49, 130-138.	0.7	5
161	Magnetic shielding of a thin Al/steel/Al composite. COMPEL - the International Journal for Computation and Mathematics in Electrical and Electronic Engineering, 2020, 39, 595-609.	0.5	5
162	Contrasting Paleoproterozoic granitoids in the Kerdous, Tagragra d'Akka, Agadir-Melloul and Iguerda inliers (western Anti-Atlas, Morocco). Journal of African Earth Sciences, 2022, 189, 104500.	0.9	5

#	Article	IF	CITATIONS
163	Study of Local Microstructure and Texture Heterogeneities in Hot Rolled CGO Fe-3%Si Sheets. Materials Science Forum, 2004, 467-470, 123-128.	0.3	4
164	Influence of Thermo-Mechanical Treatments on the Stored Energy Simulated by FEM for Two Low Carbon Steels. Materials Science Forum, 2005, 495-497, 1291-1296.	0.3	4
165	Evolution of Microstructure and Texture during Annealing of a Copper Processed by ECAE. Materials Science Forum, 2005, 495-497, 845-850.	0.3	4
166	Electron Backscattered Diffraction of Transgranular Crack Propagation in Soft Steel. Chinese Physics Letters, 2007, 24, 1759-1762.	1.3	4
167	Dynamic Recrystallization Mechanisms on Spot Welding of 6008 Aluminium Alloy to Steel by Friction Stir Welding. Materials Science Forum, 2007, 558-559, 477-483.	0.3	4
168	Evolution of Mechanical and Electrical Properties During Annealing of the Copper Wire Drawn. , 2011, , $\cdot$		4
169	Investigation of the relationships between mechanical properties and microstructure in a Fe-9%Cr ODS steel. EPJ Nuclear Sciences & Technologies, 2016, 2, 7.	0.3	4
170	Microtextural Changes and Superplasticity in an Al-7075 Alloy Processed by High-Pressure Torsion. Materials Science Forum, 2016, 838-839, 445-450.	0.3	4
171	Microstructure, Texture, and Mechanical Properties of Ni-W Alloy After Accumulative Roll Bonding. Journal of Materials Engineering and Performance, 2018, 27, 5561-5570.	1.2	4
172	Continuous Severe Plastic Deformation of Low arbon Steel: Physical–Mechanical Properties and Multiscale Structure Analysis. Steel Research International, 2021, 92, 2000482.	1.0	4
173	Study of texture, mechanical and electrical properties of cold drawn AGS alloy wire. Steel and Composite Structures, 2016, 22, 745-752.	1.3	4
174	Caractérisation de la texture de recristallisation primaire et de la spécialité des joints de grains de tÃ1es de Fe-3%Si par diffraction des electrons rétrodiffusés. Journal of Applied Crystallography, 1992, 25, 400-408.	1.9	3
175	Recrystallization Texture in Fe 3% Si Alloys Obtained by Direct Casting: Characterization by EBSD and X-Ray Diffraction. Materials Science Forum, 1994, 157-162, 1027-1032.	0.3	3
176	Estimation des déformations par diffraction des électrons rétrodiffusés. Revue De Metallurgie, 1998, 95, 611-620.	0.3	3
177	Influence of Oxygen Content on the Static Recrystallization of ETP Copper. Materials Science Forum, 2004, 467-470, 471-476.	0.3	3
178	Recovery and Recrystallization Study after Low Deformation Amount by Cold Rolling in an IF-Ti Steel. Materials Science Forum, 2004, 467-470, 183-188.	0.3	3
179	Recrystallization Mechanisms in Wire-Drawn Copper. Materials Science Forum, 2004, 467-470, 135-140.	0.3	3
180	Effect of Strain Path on Microstructure and Texture Development in ECAP Processed AA3104 Alloy. Solid State Phenomena, 2010, 160, 265-272.	0.3	3

#	Article	IF	CITATIONS
181	EBSD study of the microstructure evolution in a commercially pure aluminium severely deformed by ECAP. IOP Conference Series: Materials Science and Engineering, 2012, 32, 012025.	0.3	3
182	Soudage homogène MIG de l'alliage d'aluminium 6061. MATEC Web of Conferences, 2013, 7, 02009.	0.1	3
183	Microstructure and Microtexture Evolution of Invar Alloy after Cross Accumulative Roll Bonding (CARB) Compared to ARB. Materials Science Forum, 0, 879, 744-749.	0.3	3
184	Preparation of metallographic specimens for electron backscatter diffraction. Emerging Materials Research, 2017, 6, 260-264.	0.4	3
185	Study of Microstructural and Mechanical Behavior of Mild Steel Wires Cold Drawn at TREFISOUD <i></i> . International Journal of Engineering Research in Africa, 2018, 36, 53-59.	0.7	3
186	Optimization of Microstructural Evolution during Laser Cladding of Ni Based Powder on GCI Glass Molds. Key Engineering Materials, 0, 813, 185-190.	0.4	3
187	SOLID STATE DIFFUSION BONDING OF X70 STEEL TO DUPLEX STAINLESS STEEL. Acta Metallurgica Slovaca, 2022, 28, 106-112.	0.3	3
188	Texture Study of Naturally Deformed Quartzites From the Betic Cordilleras (Spain). Textures and Microstructures, 1991, 14, 371-376.	0.2	2
189	Determination of the total texture function from individual orientations modelled by a Lorentzian distribution. Journal of Applied Crystallography, 1993, 26, 207-213.	1.9	2
190	Microtexture Characterization by EBSP in Iron and Titanium Alloys. Textures and Microstructures, 1993, 20, 165-177.	0.2	2
191	Neutron diffraction study of the cube texture development in FeNi53% alloy. Physica B: Condensed Matter, 2000, 276-278, 914-915.	1.3	2
192	Microstructure and Texture Analysis in a Cold-Rolled Austenitic-Ferritic Steel with Duplex Structure. Materials Science Forum, 2002, 408-412, 1359-1364.	0.3	2
193	Simulation of recrystallization starting from microstructures characterized by TEM or by OIM\$^{{m TM}}\$. Application to Fe-3%Si and Fe-36%Ni alloys. Revue De Metallurgie, 2002, 99, 121-134.	0.3	2
194	Monte Carlo Modelling of Recrystallization Mechanisms in Wire-Drawn Copper from EBSD Data. Materials Science Forum, 2004, 467-470, 635-640.	0.3	2
195	Texture of Al-Cu Alloys Deformed by ECAP. Materials Science Forum, 2005, 495-497, 851-856.	0.3	2
196	Characterization of Global and Local Textures in Hot Rolled CGO Fe3%Si. Materials Science Forum, 2006, 509, 25-30.	0.3	2
197	Multiscale Approach to Texture-Microstructure Coupling. Materials Science Forum, 2006, 509, 1-10.	0.3	2
198	Role of Recovery in the Recrystallization Simulation Application to a Cold Rolled IF-Ti Steel and a Cold Drawn Copper Wire. Materials Science Forum, 2007, 550, 453-458.	0.3	2

#	Article	IF	CITATIONS
199	Stored Energy Characterization after Low Deformation by Rolling or Tension of an IF-Ti. Materials Science Forum, 2007, 558-559, 323-328.	0.3	2
200	Characterisation of transgranular crack propagation by EBSD in a soft steel. Journal of Physics: Conference Series, 2010, 240, 012036.	0.3	2
201	Some Major Features in Texture and Anisotropy Field. Advanced Engineering Materials, 2010, 12, 967-970.	1.6	2
202	Texture and Microstructure of Invar <sup>®</sup> Deformed by Asymmetrical Rolling. Materials Science Forum, 2010, 636-637, 538-543.	0.3	2
203	Microstructural Evolution Modelling of Nickel Base Superalloy during Forging. Materials Science Forum, 0, 636-637, 624-630.	0.3	2
204	Generalized Pole Figures and Stored Energy Distribution Function Obtained by X-Ray Diffraction. Materials Science Forum, 0, 702-703, 519-522.	0.3	2
205	Microstructure and Texture Evolutions in AA1200 Aluminum Alloy Deformed by Accumulative Roll Bonding Method. Solid State Phenomena, 0, 186, 112-115.	0.3	2
206	Glass and glass-ceramics along the SrTiO3-NaPO3line. MATEC Web of Conferences, 2013, 5, 04013.	0.1	2
207	Orientation changes near the interface of explosively bonded (carbon steel)/Zr700 sheets. IOP Conference Series: Materials Science and Engineering, 2015, 82, 012056.	0.3	2
208	Tem Study of Recrystallization in Ultra-Fine Grain AA3104 Alloy Processed by High-Pressure Torsion. Archives of Metallurgy and Materials, 2015, 60, 131-144.	0.6	2
209	Development of an in situ method for measuring elastic and total strain fields at the grain scale with an estimation of accuracy. Journal of Materials Science, 2016, 51, 1234-1250.	1.7	2
210	Magnetostrictive and magnetic effects in Fe-27%Co laminations. AIP Advances, 2018, 8, 047711.	0.6	2
211	Low cycle fatigue of 316L stainless steel processed by surface mechanical attrition treatment (SMAT). MATEC Web of Conferences, 2018, 165, 15002.	0.1	2
212	On the groove pressing of Ni-W alloy: microstructure, texture and mechanical properties evolution. Metallic Materials, 2018, 56, 313-323.	0.2	2
213	Multiscale modeling of a low magnetostrictive Fe-27wt%Co-0.5wt%Cr alloy. AIP Advances, 2018, 8, .	0.6	2
214	Texture, microstructure and mechanical properties evolution in Fe-x (x = 36 and 48 wt.%) Ni alloy after accumulative roll bonding. IOP Conference Series: Materials Science and Engineering, 2018, 375, 012034.	0.3	2
215	Cr cluster characterization in Cu-Cr-Zr alloy after ECAP processing and aging using SANS and HAADF-STEM. Metallic Materials, 2020, 57, 121-129.	0.2	2
216	Texture and Microstructure Evolution in a Fe-Si CGO Sheet during the Processing Route before Secondary Recrystallization. Ceramic Transactions, 0, , 123-130.	0.1	2

#	Article	IF	CITATIONS
217	A Study of Local Microstructure and Texture Heterogeneities in a CGO Fe3%Si Alloy from Hot Rolling to Primary Recrystallization. Materials Science Forum, 0, , 483-488.	0.3	2
218	Polycrystalline Modelling of Udimet 720 Forging. , 2008, , .		2
219	Direct Correspondence between the Volumic Fractions Found by Texture Analysis with the Vector Method and the Harmonic Method and Inverse Correspondence. Materials Science Forum, 1994, 157-162, 459-464.	0.3	1
220	Grain Growth Simulation by Monte Carlo Method in a HiB Fe 3% Si Alloy. Materials Science Forum, 1994, 157-162, 1847-1854.	0.3	1
221	Semiautomatic measurement of individual orientation of crystals by using etch pits and digitized images. Materials Characterization, 1995, 34, 189-194.	1.9	1
222	Etude de la recristallisation d'un monocristal de cuivre d'orientation (112)[ll1] déformé à tempéra ambiante en compression plane imposée. Revue De Metallurgie, 1997, 94, 1057-1062.	ture 0.3	1
223	Effect of Deformation Path on Torsion Texture and Stored Energy of Copper Rods. Materials Science Forum, 2002, 408-412, 625-630.	0.3	1
224	Neutron Diffraction Study of Texture and Stored Energy in ECA Pressed Copper. Materials Science Forum, 2002, 408-412, 703-708.	0.3	1
225	A Method of Determination of Stored Energy in Single and Dual Phase Cold Rolled Materials. Materials Science Forum, 2002, 408-412, 583-588.	0.3	1
226	EBSD Study of Annealing Twinning during Recrystallization of Cold Rolled Copper. Materials Science Forum, 2005, 495-497, 1303-1308.	0.3	1
227	Bringing Mobility to Synchronous Collaborative Activities: Recent Enhancements of the "Platine" Platform. , 0, , .		1
228	Friction stir welding: a process for obtaining bimetallic welds. Welding International, 2008, 22, 90-99.	0.3	1
229	Structural and Dielectric Properties of BaTiO3-NaPO3 Glass-Ceramics. Ferroelectrics, 2008, 371, 56-62.	0.3	1
230	Formation and Development of Strong Cube Recrystallization Texture in an Aluminium of Commercial Purity. Materials Science Forum, 2011, 702-703, 391-397.	0.3	1
231	An Investigation of Microtexture Evolution in an AlMgSi Alloy Processed by High-Pressure Torsion. Materials Science Forum, 0, 702-703, 165-168.	0.3	1
232	Nucleation of Recrystallization in Fine Grained AA3104 Alloy Analyzed by SEM and TEM Orientation Mappings. Materials Science Forum, 0, 702-703, 324-327.	0.3	1
233	Dynamic Recrystallization in Similar 5182 Al/Al and Dissimilar Al/Fe Friction Stir Spot Welds. Materials Science Forum, 2012, 715-716, 152-157.	0.3	1
234	Multi-scale analysis by SEM, EBSD and X-ray diffraction of deformation textures of a copper wire drawn industrially. MATEC Web of Conferences, 2013, 5, 04004.	0.1	1

#	Article	IF	CITATIONS
235	Texture in Welded Industrial Aluminum. Applied Mechanics and Materials, 0, 563, 7-12.	0.2	1
236	Measurement of Complementary Strain Fields at the Grain Scale. Advanced Materials Research, 0, 996, 64-69.	0.3	1
237	Effect of microalloying elements on the Cube texture formation of Fe48%Ni alloy tapes. IOP Conference Series: Materials Science and Engineering, 2015, 82, 012036.	0.3	1
238	Texture Gradient through Thickness of a Cross Roll-Bonded AA5754/AA6061 Aluminum Composite. Materials Science Forum, 0, 879, 2038-2043.	0.3	1
239	Deformation and Recrystallised Texture Evolution and the Followed Mechanical and Electrical Properties of Drawn and Annealed Copper Wires. International Journal of Engineering Research in Africa, 2017, 31, 20-28.	0.7	1
240	Origin of the {111}〈112〉 Cold Rolling Texture Development in a Soft Magnetic Fe-27%Co Alloy. Journal of Materials Engineering and Performance, 2019, 28, 3767-3776.	1.2	1
241	Effect of the hot rolling on Goss development and magnetic induction in an advanced soft magnetic Fe–27%Co alloy. Journal of Alloys and Compounds, 2020, 834, 155149.	2.8	1
242	Wire Drawing Effect on Microstructural and Textural Evolution in Medium Carbon Steel Wires. Defect and Diffusion Forum, 0, 406, 505-510.	0.4	1
243	Multi-Scale Characterization by Neutronography and Electron Diffraction of Ni Coating on Cu-Ni-Al or Cast-Iron Glass Molds after Laser Cladding. Materials Science Forum, 0, 1016, 297-302.	0.3	1
244	An evaluation of high temperature tensile properties for a magnesium AZ31 alloy processed by high-pressure torsion. Letters on Materials, 2015, 5, 341-346.	0.2	1
245	Texture Evolution in Invar <sup>®</sup> Deformed by Asymmetrical Rolling. Materials Science Forum, 0, , 551-556.	0.3	1
246	Characterization of Global and Local Textures in Hot Rolled CGO Fe3%Si. Materials Science Forum, 0, , 25-30.	0.3	1
247	Shear impact during steel wire drawing on grain boundaries and mechanical properties. Letters on Materials, 2020, 10, 558-565.	0.2	1
248	Investigation of residual strain in quartzite using neutron diffraction: Interpretation and selfâ€consistent modelling. Geological Journal, 2022, 57, 1125-1136.	0.6	1
249	Microstructure and texture evolution of ECAP-processed Mg-Ce alloy during isothermal annealing. Materials Today Communications, 2022, 32, 103920.	0.9	1
250	Deformation Textures: Connection Between Modelling and Experience in Elastoplastic Behaviour of Polycrystals. Textures and Microstructures, 1991, 14, 1115-1120.	0.2	0
251	Etude microstructurale d'un revêtement déposé par arc plasma semi-transféré sollicité en fatigue thermique. Revue De Metallurgie, 1993, 90, 1691-1702.	0.3	0
252	Simulation of Rolling and Deep Drawing Textures in Ferritic Steels: Application to Ear Profile Calculation in Deep Drawing. Materials Science Forum, 1994, 157-162, 1739-1746.	0.3	0

#	Article	IF	CITATIONS
253	Local Orientation Changes during Shear Banding of Copper Single Crystals Compressed in Channel-Die. Materials Science Forum, 1994, 157-162, 1237-1242.	0.3	0
254	Modélisation et Simulation de la Croissance de grains et de la recristallisation primaire. European Physical Journal Special Topics, 1995, 05, C3-51-C3-66.	0.2	0
255	Simulation et Caractérisation des Textures de Recristallisation d'un Alliage Fer 3% de Silicium Obtenu par Coulée Directe en Bande Mince. European Physical Journal Special Topics, 1995, 05, C3-77-C3-86.	0.2	0
256	Texture in 3% Si-Fe Ribbon Cast Directly. Materials Science Forum, 1996, 204-206, 121-132.	0.3	0
257	On critical polyhedrons for B.C.C. and H.C.P. materials. International Journal of Plasticity, 1999, 15, 209-222.	4.1	0
258	Influence of the Goss Grain Neighbourhood during Secondary Recrystallization of Fe-3%Si Sheets. Materials Science Forum, 2002, 408-412, 1251-1256.	0.3	0
259	Recrystallization Study of a Low Carbon Steel after Tensile Strain. Materials Science Forum, 2003, 426-432, 3649-3654.	0.3	0
260	Stored energy evolution as a function of cold rolling reduction for a Fe-53%Ni alloy and an austenitic-ferritic steel. Revue De Metallurgie, 2003, 100, 851-858.	0.3	0
261	Neutron and X-ray diffraction study of Al and Cu during ECA processing and subsequent recrystallization. Revue De Metallurgie, 2003, 100, 825-833.	0.3	0
262	Monte Carlo Modelling of Recrystallization Process in Cold Rolled IF-Ti Steel. Materials Science Forum, 2004, 467-470, 665-670.	0.3	0
263	Recrystallization in an IF-Ti Steel after Low Deformation Amount by Tensile Strain. Materials Science Forum, 2005, 495-497, 1297-1302.	0.3	0
264	Monte Carlo Simulation of Grain Growth in Feâ€3 % Si Steels by Consideration of a Morphological Parameter. Advanced Engineering Materials, 2010, 12, 1015-1017.	1.6	0
265	Crystallographic Texture Control Helps Improve Pipeline Steel Resistance to Hydrogen-Induced Cracking. , 2010, , .		0
266	EBSD Study of Grain Boundary Evolution after Different Cold Rolling Reduction in Duplex Steel. Materials Science Forum, 2010, 636-637, 504-510.	0.3	0
267	Study of Refined Microstructures after Two-Step Heat Treatments by Means of EBSD Technique on γ-TiAl Alloys. Materials Science Forum, 2010, 638-642, 1416-1421.	0.3	0
268	Texture Evolution of Armco Iron during Accumulative Roll Bonding Process. Materials Science Forum, 0, 702-703, 177-181.	0.3	0
269	Microstructure and Texture Evolution of a Cold Rolled Ni-Cr-W Alloy after Annealing. Materials Science Forum, 0, 702-703, 352-355.	0.3	0
270	Evaluation Of Four Welding Arc Processes Applied To 6061 Aluminium Alloy. , 2011, , .		0

Evaluation Of Four Welding Arc Processes Applied To 6061 Aluminium Alloy. , 2011, , . 270

#	Article	IF	CITATIONS
271	Microstructure Evolution during the Accumulative Roll Bonding Process in Armco Iron. Materials Science Forum, 0, 706-709, 1757-1762.	0.3	0
272	Crystallographic Aspects of Deformation and Recrystallization in ECAP-Processed AA3104 Aluminium Alloy. Solid State Phenomena, 0, 186, 98-103.	0.3	0
273	Recrystallization in Ultra-Fine Grain Structures of AA3104 Alloy Processed by ECAP and HPT. Materials Science Forum, 0, 715-716, 346-353.	0.3	Ο
274	SEM-EBSD Observations of Crack Initiation and Propagation due to Orientation Changes during Forming in Mild Steel. Advanced Materials Research, 0, 682, 25-32.	0.3	0
275	Recrystallization of ECAP-Processed AA4343 Aluminium Alloy Containing Large Second Phase Particles. Materials Science Forum, 2013, 753, 239-242.	0.3	Ο
276	Recrystallization and Grain Growth due to Annealing of an Ultrafine-Grained Al Alloy. Materials Science Forum, 2013, 753, 303-306.	0.3	0
277	Copper Refinement from Anode to Cathode and then to Wire Rod: Effects of Impurities on Recrystallization Kinetics and Wire Ductility. Microscopy and Microanalysis, 2015, 21, 1153-1166.	0.2	0
278	In memoriam tribute to Richard Penelle (1936-2012). IOP Conference Series: Materials Science and Engineering, 2015, 82, 011002.	0.3	0
279	Recrystallization and grain growth at the interface of a bimetallic colaminated strip composed of two different Fe-Ni alloys. Journal of Physics: Conference Series, 2019, 1270, 012024.	0.3	Ο
280	Microstructural peculiarities and textural characteristics of Ni–W sheet alloy after accumulative roll-bonding and annealing. SN Applied Sciences, 2020, 2, 1.	1.5	0
281	On the Influence of Crystallographic Texture on HIC. , 2006, , .		Ο
282	A Monte-Carlo Algorithm for the Zener Drag Effect in the Fe-3%Si Magnetic Alloys. Ceramic Transactions, 0, , 251-256.	0.1	0
283	Textural Inhomogeneity Effect during the Monte Carlo Simulation of the Abnormal Goss Grain Growth in Fe-3%Si Steel Grade HiB. Ceramic Transactions, 0, , 365-372.	0.1	0
284	Hydrogen-Induced Crack Interaction and Coalescence: The Role of Local Crystallographic Texture. , 2010, , .		0
285	Caractérisation de la Texture de Recristallisation Primaire d'une Tole de Fe3%Si (Nuance HiB). European Physical Journal Special Topics, 1995, 05, C3-285-C3-290.	0.2	Ο
286	Evolution de la texture et de la microstructure d'un aluminiure de titane biphase γ/ α <sub>2</sub> en fonction des traitements thermiques. European Physical Journal Special Topics, 1996, 06, C2-235-C2-240.	0.2	0
287	Intermetallic Texture Analysis by X-Ray, Neutron and Electron Backscattered Diffraction. European Physical Journal Special Topics, 1996, 06, C2-141-C2-146.	0.2	Ο
288	Analyse des textures cristallographiques et des microstructures. , 2015, , 80-85.	0.1	0